HYDROMETEOR AND LATENT HEAT PROFILES OF TROPICAL CYCLONES CONSON, IVAN AND CATARINA USING PR/TRMM DATA

Marcelo Rosa Barbio[1]

Augusto José Pereira Filho[2]

and

Prakki Satyamurty[1]

1 – Centro de Previsão de Tempo e Estudos Climáticos (CPTEC) – Instituto Nacional de Pesquisas Espaciais (INPE), km 40, Rodovia Presidente Dutra, Cachoeira Paulista, SP, Brazil.

2 – Instituto de Astronomia, Geofísico e Ciências Atmosféricas (IAG) – Universidade de São Paulo (USP), Rua do Matão, 1226, São Paulo, SP, Brazil.

Abstract

Microphysical and thermodynamical features of three tropical systems, namely Hurricanes Ivan and Catarina (Brazil) and Conson Typhoon are analyzed based on space-born radar measurements available on the TRMM satellite. A more detailed analysis is performed for Hurricane Catarina, the first of its kind, observed with new high spatial and temporal resolution data sets. A hydrometeor classification procedure was used to estimate vertical profiles of latent heating rates associated with them. High mean water content was found in Conson and Ivan at low levels and close to their centers. Results indicate that hurricane Catarina was shallower than the other two systems with less water, concentrated closer to its center. The mean ice content in Catarina was about 0.05 g kg^{-1} while in Conson it was 0.06 g kg^{-1} and in Ivan 0.08 g kg^{-1}. Conson and Ivan had water content up to 0.3 g kg^{-1} above the melting layer, while Catarina had less than 0.15 g kg^{-1}. All the three systems presented warm air at higher levels near the eye as a consequence of heating, probably caused by diabatic compression and/or latent heat release.

1 – Introduction

Hurricanes are the strongest atmospheric systems that develop in tropical atmosphere. Normally, these systems are generated north of the ITCZ as a perturbation in the easterly current. Initially appearing as a thunderstorm cluster, the perturbation becomes a tropical depression by gaining energy through release of latent heat by conversion of vapor into droplets. If the SST is warmer than 26.5°C, the depression develops an eye and receives the name of hurricane. This is a typical sequence. However, not all hurricanes are generated and grown over the tropical oceans. There are cyclones which are generated as mesoscale systems away from the tropics, like those occurring in the coast of Australia (Holland et al. 1987) and, recently, near the Brazilian coast. The Brazilian cyclone in the South Atlantic and two other tropical cyclones, one in the North Atlantic and the other in the North Pacific, are the subject matter of the present study, with special emphasis on the first, which was a rare event in the South Atlantic. The three cyclones are fairly recent ones.

The main objective of this work is to analyze hydrometeors and latent heating fields of the three tropical cyclones. 3D reflectivity fields of the Precipitation Radar (PR) of the Tropical Rainfall Measurement Mission (TRMM) satellite (Kummerow et al. 1998) are used to develop a model of hydrometeor distribution and concentration within the tropical systems. The hydrometeors are classified as precipitating (i.e., hail, graupel, snow and rain) and non-precipitating (i.e., ice crystals and cloud water). Precipitation is further classified as stratiform and convective to improve the dispersion relation (Iguchi et al. 2000) and the quantification of heating rate and cooling rate fields due to phase change (Brown 1979, Leary and Houze 1979, Lang et al. 2003). The energy released in this process is very important for the large-scale circulation (Silva Dias et al. 1983, De Maria 1985, Gandu and Geisler 1991, Gandu and Silva Dias 1998, Yanai and Tomita 1998).

The hydrometeor profiles are obtained using the correlations between the SPOL estimates and the PR/TRMM signal over the state of Rondonia, Brazil, during LBA/TRMM experiment (Large Scale Biosphere Atmosphere Interaction/Tropical Rainfall Measuring Mission) between January and February of 1999.

The classification of the hydrometeors into convective and stratiform is obtained with PR/TRMM 2A23 product through its vertical distribution (Heymsfield et al. 2000), named method H for the Ku

radar, and horizontal distribution (Steiner et al. 1995). The first one compares a given signal intensity to the average signal intensity of the surrounding background below the melting layer, around 3 km altitude. Cells with reflectivity above 40 dBz are classified as convective. If the reflectivity is below 40 dBz the cell reflectivity must be at least 4.5 dBz higher than the background to be considered as convective cell. The second method classifies the cloud based on its vertical structure. If a bright band (BB) is detected, it is classified as stratiform. The latent heat release is estimated using the model developed by Tao et al. (1990), which is based on the vertical fluxes of hydrometeors of precipitating and non-precipitating systems.

2 - Methodology

Hydrometeor types and respective contents were estimated from SPOL weather radar polarimetric measurements obtained during the LBA/TRMM experiment (Large Scale Biosphere Atmosphere Interaction/Tropical Rainfall Measuring Mission) in Rondonia, Brazil between January and February of 1999 (Silva Dias et al. 2002). These estimates serve as reference values. The hydrometeor classification was performed with a fuzzy logic method (Rocco 2003). Unfortunately, only four overpasses of the TRMM coincided with significant convection within 100 km of the SPOL radar surveillance area during the experiment. Vertical profiles of reflectivity for both SPOL and TRMM Ku band Precipitation Radar (PR) measurements are compared. As pointed out by Bolen and Chandrasekar (2000) any quantitative cross validation point-to-point between the nonattenuating ground radar (SPOL) and attenuating space borne radar (PR), must ensure that both are well calibrated. However, even considering that the correlation between the two sets of radars is simple in thesis, it is difficult to accomplish in practice. Specially, inaccuracies due differences in sampling strategies and synchronization or variations in the satellite orbital parameters could result in wrongs scattergrams. So, an alternative method is to use space average of the reflectivities. This methodology mitigate problems related to PR missing echoes, which lost all signal below 14,0 dBz resulting in an underestimation of 3.8% of surface rain, negligible if compared to accuracy of precipitation. And, in situations with low or absent attenuation the reflectivities agree within 1dB.

Anagnostou et al. (2001) indicate that the reflectivity measurement differences of ground based radars and the PR/TRMM are independent of the signal intensity with a negative bias. A linear correction

function was applied to the PR data based on constant altitude plan position indicator (CAPPI) reflectivity fields of SPOL and PR:

$$Z_{pr} = \beta Z_{spol} \quad (1)$$

where, Z_{pr} and Z_{spol} are reflectivities (dBz) measured by the PR/TRMM and the SPOL radar, respectively, and β is a constant. This constant is determined by using Rondonia data sets. Eq. 1 was obtained for convective and stratiform precipitating systems separately. The relationship was applied to all SPOL data (about 200 volume scans in two months). The adjusted data was used as a simulation of a Ku band PR/TRMM radar.

The adjusted and original fields of hydrometeors were again correlated using the disdrometer drop size distribution (DSD) function to estimate the hydrometeor contents (Lilly 1964, Smith Jr et al. 1975, Smith Jr 1984):

$$W_h = aZ_{pr}^b \quad (2)$$

where, W_h is the space average hydrometeor mass content (liquid or frozen) in g kg^{-1} derived from SPOL, and *a* and *b* are parameters determined by best-fitting adjustment. Eq. 2 is used to estimate ice content above the melting layer or bright band (BB) when that is detected and liquid water content below it. The parameters *a* and *b* in these two cases are different and are also different for convective and stratiform areas.

The above equation is not applied when there is mixture of water and ice. In this case, the liquid water content is computed from the method used to estimate the rainfall rate for PR/TRMM by Iguchi et al. (2000). In this method, about 500 m above the BB, or 750 m above the melting level when BB is not detected, the liquid water content, compared to the total content (liquid + ice), is adjusted to be 17%. At the cloud top it is reduced to only 1.1%. These percentages are used to estimate the liquid water content.

To estimate the ice content below the 0 °C isotherm, we assume that the heat used by melting cools the environment by evaporation of liquid water produced at the surface of graupel or snow. The rate of mass loss of ice is estimated from the following equation (Smith Jr et al. 1975):

$$L_i + c_w T \frac{dm}{dt} = 2\pi D_g f(\mathrm{Re}) K_T T - L_v D_v \Delta\rho \quad (3)$$

where L_i is latent heat of fusion (J kg^{-1}); C_w is thermal conductivity of water (J kg^{-1}K^{-1}); L_v is latent heat of evaporation (J kg^{-1}); D_v is diffusivity of water vapor (m^{-2} s^{-1}); K_T is heat diffusivity (J m^{-1} s^{-1} K^{-1}); D_g is diameter of graupel or snow (m); $\Delta\rho$ is difference of density between air at the surface of hydrometeor and the air away from it at a large distance (kg m^{-3}); f(Re) is Reynolds ventilation factor.

The total mass of graupel and snow has an exponential distribution with an interception parameter N_0=0.04 cm^{-4} (Smith Jr 1975). The ice crystal distribution is similar to the one given in Heymsfield (2003) in which ice particle properties are analyzed through radiosondes and aircraft probes flying in tropical and mid-latitude regions. He used a normalized gamma distribution, following Dou et al. (1999). With the above methods, it is possible to estimate the total mass of graupel and snow and non-precipitating ice crystals, separately.

The same methodology is used to compute rainwater and cloud water contents by using a gamma function with μ (parameter determining the position of maximum concentration of hydrometeor) obtained from profiles of rainwater and cloud water with the TMI (TRMM Microwave Imager) sensor aboard the TRMM satellite. The rainwater and cloud water contents estimated by TMI sensor are averaged over the area covered by the SPOL radar. Furthermore, the horizontal ratio of rainwater and cloud water in each level derived from this sensor is used as a parameter of DSD convergence integrated in the range of cloud drops (D_{10} and D_{240}) and rain drops (D_{240} and D_{5000}) as given below:

$$\frac{W_n}{W_c} = \frac{\sum_{D_0}^{D_{240}} \kappa(D,\mu) D^{\mu} e^{-\lambda D}}{\sum_{D_{240}}^{D_{5000}} \kappa(D,\mu) D^{\mu} e^{-\lambda D}} \quad (4)$$

where W_n is horizontal mean cloud water content from TMI (kg kg^{-1}); W_c is horizontal mean rain water content from TMI (kg kg^{-1}); D_{10} is minimum diameter of a cloud droplet (cm); D_{240} is minimum diameter of a small drop (cm); D_{5000} is maximum diameter of a drop (cm).

The parameters κ on the right-side of Eq. 4 are gamma functions. The slope parameter λ is defined as in Ulbrich (1983). With the help of Eq. 4 one can determine a μ for each isothermal level, giving one solution for the ratio between the rain and cloud contents. Ulbrich (1983) showed that there is a relationship between N_0 and μ. Later, Chandrasekar and Bringi (1987) indicated that the relationship is

unstable and depends on the adjustment method, thus limiting its utility. Moreover, Viltard et al. (2000) used PR/TRMM data to estimate the interception parameter N_0 for convective and stratiform clouds, which are found to be 0.017 cm^{-4} and 0.048 cm^{-4}, respectively.

Tao et al. (1990) have developed a model to estimate the rate of latent heat release based on vertical fluxes of precipitating hydrometeors (rain and aggregates):

$$\frac{dT}{dt} = -\frac{L}{c_p} V_i \frac{dw_i}{dz} \tag{5}$$

where, L is latent heat of condensation (J kg^{-1}); c_p is specific heat (J $kg^{-1}K^{-1}$); w_i is hydrometeor content (kg kg^{-1}); V is terminal velocity (m s^{-1}) of the rain or the aggregate, given by:

$$V_i = \frac{\mathrm{Re}\eta}{D_i \rho} \tag{6}$$

where Re is Reynolds number; η is dynamical viscosity (kg m^{-1} s^{-1}); ρ is a density of air (Kg m^{-3}); D_i is diameter of the hydrometeor (m).

According to Beard e Grover (1974), the Reynolds number for a drop of diameter can be written as:

$$\mathrm{Re} = \exp(F) \tag{7}$$

where F is a cubic function given by:

(8)

and x as:

$$x = \ln\left[\frac{32}{3}\frac{(\rho_a - \rho)\rho g}{\eta^2} D_i^3\right] \tag{9}$$

where ρ_a is the density of the hydrometeor; and g is the gravity. The parameter in Eqs. 7 to 9 are in all cgs units.

If dw_i/dz in Eq. 5 is negative (positive), there is condensation (evaporation) or deposition (sublimation) or conversion to aggregates of a more complex microphysical structure. In this study

heating and cooling due to rain will be labeled Rcond and Evap, respectively. Lang et al. (2003) showed, using data obtained during PRE-STORM (*Preliminary Regional Experiment for Storm Scale Operational and Research Meteorology*) experiment and TOGA/COARE (*The Tropical Ocean Global Atmosphere Coupled Ocean Atmosphere Response Experiment*), that between 4 and 6 km altitude freezing is the most important process. But, between 6 and 9 km the deposition is predominant. For large aggregates at this level, the mass increase is due to the collection of ice crystals and super-cooled water (Tao et al. 1990; Lang et al. 2003), especially within convective regions (Olson et al. 2006) where raindrops are abundant.

As a first approximation, the latent heat release caused by deposition/freezing is linearly proportional to the concentration of ice crystals/drops. Eq. 5 for aggregate precipitation takes the form:

$$\frac{dT}{dt} = -\frac{L_s}{c_p} corr + L_f (1 - corr) \frac{V}{c_p} \frac{dm}{dz} \tag{10}$$

where V is the terminal velocity of the aggregate and the proportion factor (corr) is given by the ratio between the ice mass and super cooled drops:

$$corr = \frac{m_i}{m_i + m_a} \tag{11}$$

where m_a is the total water content (cloud and rain water, kg kg^{-1}), m_i is the ice content and L_s and L_f are the latent heats of sublimation and fusion, respectively. The first term in Eq. 10 represents the heating rate by deposition of vapor over aggregates. The second is related to freezing of super-cooled water drops caught by aggregates. The heating due to the aggregate flux will be labeled Dep and cooling due to melting, Melt. Eq. 11 is a first approximation and further studies are required for the verification of its suitability.

For the non-precipitating cloud water and ice crystals, only part of the total mass is used to heat the atmosphere:

$$\frac{dT_i}{dt} = 0{,}5 \frac{L_i}{c_p} coef(\overline{w}_i) \tag{12}$$

The *coef* is 0.15 in Tao et al. (1990). This parameter is estimated by Tao et al. (1994) from the amount of precipitation reaching the ground, as given below:

$$coef = \frac{\frac{L_v}{c_p} P_0 - \int_{base}^{top} \rho \frac{dT}{dt} \Delta z}{\int_{base}^{top} \rho \left(\frac{L_v}{c_p} q_n + \frac{L_s}{c_p} q_c \right) \Delta_z} \qquad (13)$$

where P_0 is precipitation rate (mm hr^{-1}). The heating due to cloud water and ice will be labeled respectively, Ccond and DepI.

Following the methodology proposed by Tao et al. (1994), the heating due to rain water (Rcond) in the stratiform region and the evaporation (Evap) in the convective region are three times less than other terms, so both can be neglected.

The total diabatic heating rate due to latent heat release is the sum of all terms given below:

$$\frac{dT}{dt} = Rcond + Ccond + dep + depI + evap + melt \equiv Total \qquad (14)$$

3 – Synoptic Overview of the Tropical Cyclones

Three tropical cyclones, one each in the North Atlantic, in the western North Pacific and the South Atlantic, are described here. The two cyclones of the Northern Hemisphere presented extraordinary strength and the third is a unique event near the Brazilian coast.

a – Typhoon Conson

The Typhoon Conson, named in homage to a province in Vietnam, was generated from a tropical storm located at 215 km east of Hong Kong, in China Sea, on 4 June 2004. On the following day, already grown into a tropical depression, Conson took a E-NE trajectory. The estimated maximum surface wind velocity at that moment was 30-35 knots. On 6 June Conson strengthened and changed its path a little heading to the north, forced by a surface ridge over the Philippine islands. On this day, the strength of the

winds was 50 knots. On 7 June the tropical depression stayed at only 195 km from southern coast of Taiwan. The system grew further in strength and, finally, received the status of typhoon, with the presence of an eye. On 8 June (Fig. 1a) Conson continued moving slowly to the north, with a mean velocity of 8 knots and a wind strength of 65 knots, with gusts of 90 knots. The diameter of the eye was of the order of 10 km.

From a single scan of TRMM, it was possible to observe two spiral bands of precipitation or legs. There was an intensely convective area at the northeastern edge of the eye, where precipitation exceeded 12 mm hr^{-1}. The convective rain profile (not shown) showed values of the order of 18 mm hr^{-1} at 1 km above the sea level. This rate decreased quickly with altitude, reaching a value of only 1 mm hr^{-1} at 6 km.

The TRMM data showed that in the stratiform sector inside the spiral bands the precipitation values were low. Below 5 km level it was 3 mm hr^{-1}. Between 4 and 5 km there was a maximum precipitation rate associated with the BB. In the neighborhood of the eye the BB stayed at an altitude of 4.6 km. Near the external edge of the typhoon BB was found at 3.9 km. This decrease of the height away from the eye toward the borders is a sign that the eye region was hotter than the spiral legs. This signature was also found in Ivan and Catarina discussed in the following subsections.

Fortunately, Conson took a NE trajectory, avoiding to hit Taiwan. On the next day the system was still growing in strength. Infrared images showed that the eye was hot. On this day Conson reached its maximum strength, with winds of the order of 95 knots. Conson maintained its typhoon characteristics during two more days, and soon after became a tropical storm.

b – Hurricane Ivan

The super-hurricane Ivan was one of the strongest tropical storm so far recorded. It reached the category 5 in the Saffir/Simpson scale. Ivan crossed the southern region of Jamaica Island on 11 September 2004 (Fig. 1b). On this day, the surface pressure at its center was estimated at 915 hPa with wind velocity of the order of 270 km hr^{-1}. On 13, the hurricane crossed the extreme western Cuba and went on to the Mexican Gulf. It still maintained category 5 intensity, with a surface pressure estimated at 912 hPa. The eye diameter was 25 km.

The rate of precipitation at 1 km altitude was 18 mm hr^{-1} and at 6.5 km it was only 2 mm hr^{-1}. This magnitude, although larger, was not very different from that estimated in Conson. But, this value was computed using the PR sensor, whose limited scan did not cover the most intense northern and

northwestern sectors of Ivan. The precipitation in its stratiform sector rate was 3-4 mm hr^{-1} and was confined to below 5 km altitude.

On the following days, Ivan gradually lost its force, but still received a classification of category 4. The trajectory was N/NW. On 16 September, as weak as category 1, the hurricane hit the coast of USA and soon it was classified as a tropical storm. The depression further advanced into the continent and dissipated completely on 24 September.

c – Hurricane Catarina

The hurricane Catarina is one of the rarest phenomena recorded so far in Brazilian waters and territory (Fig. 1c). Thus, it is among the most interesting events of the globe. The hurricane received its name because it hit Santa Catarina State of Brazil. This tropical cyclone was formed of an extratropical cyclone and had a short lifetime, no more than a week. It hit the Brazilian coast on 29 March 2004 and caused damage of property (~500 mi USD) and loss of human lives (Gusso 2004). This storm received the status of category 1-2 hurricane.

The TRMM satellite scanned Catarina three times. The first scan was made during the formative stage (24 March 2004) and the second and third ones during the mature stage (two times on day 27 March 2004). In these last two passages the eye of the hurricane was found well developed.

Catarina first appeared as a perturbation in the South Atlantic Convergence Zone (SACZ) region under a low-over-high block (Pereira Filho and Lima 2006). This perturbation was somewhat similar to those found in the east coast of Australia (Holland et al. 1987), however, never observed in the Brazilian coast. On 27 March, in the morning hours, the TRMM scanned showed that it was possible to see an eye, with a mean diameter of 55 km, and a region of strong convection at the southern edge of this eye. There were no measurements of the surface pressure inside the eye, but estimates gave 979 hPa (Mattos and Satyamurty 2004; Calearo et al. 2004). The wind velocity was estimated to be 120 to 150 km hr^{-1}.

The hurricane arrived at the coast of Santa Catarina State in the night of 28 March. Some meteorological stations recorded wind speeds of the order of 100 km hr^{-1}, from the southern quadrant. Afterwards the direction changed to north, but with stronger force (150 km hr^{-1}) (Calearo et al. 2004).

4 – Hydrometeor Profiles in the Cyclones

The relation between the SPOL and PR data sets (Eq. 1) over Rondonia shows that they are highly correlated and the line of best fit has an inclination very close to 1.0. Table 1 shows the statistics for the convective and stratiform regions and for liquid hydrometeors and solid hydrometeors. The correlation coefficients are higher than 0.8 in all the four cases, and it is highest for the liquid hydrometeors in the convective region. The inclination of the regression line is nearly 1.0 but slightly more inclined, in the sense that the SPOL values vary somewhat slowly compared to the variation in PR reflectivity. The standard deviations are smaller in the case of liquid hydrometeors at around 2 to 3 dBz whereas for the solid hydrometeors the standard deviation was larger, reaching nearly 5.2 dBz in convective regions. SPOL data presented slightly higher values of standard deviation. The statistics are generated with the help of area means over 200 km diameter around SPOL radar, rather than point values of the reflectivities, as is mentioned in the methodology section. The sizes of the samples used were reduced to about 20, as there are data for only four days. On the whole, the statistics in the table show considerable consistency between the two datasets, which allows us to use the PR/TRMM data for studying the hydrometeor profiles.

Table 1 – Statistical relation between the reflectivities obtained by SPOL and PR

	Liquid Hydrometeors		**Frozen Hydrometeors**	
	Convective	**Stratiform**	**Convective**	**Stratiform**
Correlation	0,908	0,877	0,895	0,819
Bias (SPOL-PR)	-0.16	-2.17	-0.95	-1,95
Inclination (β)	1,003	1,091	1,018	1,065
σ(SPOL)	2,78	2,52	5,19	4,04
σ(PR)	2,06	2,54	3,33	3,57

The inclination parameter β is used to adjust the reflectivies of SPOL/PR at all the points of the SPOL for the 200 volume scans during two months (Jan-Feb 1999). Eq. 2 is used with these new data sets and the hydrometeor profiles provided by TRMM to estimate the constants *a* and *b* for convective and stratiform regions and for liquid and frozen hydrometeors. Table 2 shows the parameters and correlations obtained. The correlation between the SPOL reflectivities and the hydrometeors derived from this data is expected to be 1.0. However, the fuzzy logic method used for the estimation of hydrometeors takes into consideration other polarimetrical variables. In the four classifications, a two-sided t-distribution at level of 97.5% of confidence showed that the correlations can't be rejected. These values of *a* and *b* are, then, used to estimate the hydrometeor profiles in the three hurricane cases.

Table 2 – Parameters *a* and *b* and correlation coefficient between the corrected SPOL reflectivity and the hydrometeor concentration

	PR/TRMM			
	***a* (10^{-3})**	***b***	**Cor**	**Sample size**
convective (liquid)	1,889	0,654	0,972	29019
stratiform (liquid)	3,024	0,539	0,993	123662
convective (frozen)	7,402	0,505	0,980	17787
stratiform (frozen)	6,262	0,509	0,986	72376

Figures 2 and 3 show hydrometeor profiles classified as convective and stratiform in Catarina, Conson and Ivan. Averages were taken azimuthally with respect to the center at the eye of each system. The distance from the center of the system is shown on the abscissa. The profiles of water and ice are shown respectively, in the left and right columns of the figures.

There is a clear difference between the three cyclones in their convective sectors (Fig. 2, left column). Conson and Ivan present much more water than Catarina. Especially in the neighborhood of the

eye this difference is large. In these regions values larger than 0.12 g kg^{-1} are found in the whole vertical column up to 5 km altitude for Conson and 5.5 km for Ivan. Probably, Ivan had even more water than shown, because PR scanned only the weakest half sector of this cyclone. Ivan showed an area with values of up to 0.3 g kg^{-1} in the whole horizontal extension of the hurricane. In Conson this value was contained in the first 90 km from the center. Catarina showed two somewhat distinct regions of liquid water in excess of 0.3 g kg^{-1}. Catarina had less water than the other two systems. The maximum values did not surpass 0.8 g kg^{-1} and were confined to three small convective towers. The minimum value (0.02 g kg^{-1}) was found above 6 km in Catarina and above 7 km in the other two.

The ice profiles (right columns of Figs. 2 and 3) show some similarities. In all the three cyclones there were greater concentrations of ice in the layers immediately above the melting level. Conson showed a large concentration of ice (~0.3 g kg^{-1}) in a narrow layer between 4.5 and 5.5 km, but with a large horizontal extension (15 to 70 km). This large ice concentration indicates strong convective columns located in this area. Ivan, due to its large extension and depth, has large amounts of ice, as high as 0.3 g kg^{-1}, between 4 and 5.5 km. Ice was found also in the very high levels, up to 9 km. This ice was typically in the form of crystals.

Catarina had less ice and was concentrated in a thin layer immediately above the melting layer. The mean concentration was 0.10 g kg^{-1} and only in one sector the values surpassed 0.2 g kg^{-1}. Although, it had less ice than Ivan and Conson, Catarina showed a relatively high concentration of crystals at 8 to 9 km altitude.

Fig. 3 is similar to Fig. 2, but for the stratiform sectors. Following the description given above, Catarina showed important differences when compared to the other two systems, especially in the depth of the water content. Ivan showed some uniformity in the distribution of water. In this hurricane values of 0.12 g kg^{-1} were found, with a large concentration in the layer between 4 and 5 km altitude as in Conson.

Conson and Catarina showed areas with concentration of water as high as 0.12 g kg^{-1}, especially between 20 and 90 km from the eye of Conson and 30 and 120 km in Catarina. But, in the latter, the line of 0.12 g kg^{-1} did not cross 4 km altitude. In all the three systems, the cloud water was concentrated immediately below the BB layer. This water was composed, basically, of large drops that had been generated by the melting of the ice of the BB (Tao et al. 1990).

The stratiform ice had a similar distribution as its convective counterpart. The magnitude and vertical distributions were very similar to convective ice. The largest concentrations were located in the neighborhood of the convective tower.

5 – Profiles of Latent Heating Released by Hydrometeor (PLHRH)

Figures 4 and 5 show profiles of azimuthally averaged latent heat released by different hydrometeor types and parameters integrated in the vertical. In the convective sector the heating/cooling due to the flux of raindrops (Rcond and Evap), condensation of cloud drops (Ccond), heating/cooling due to vertical flux of frozen aggregates (Dep/Melt), and heating due to deposition to form crystals (DepI) were calculated.

Fig. 4 shows only the four most important terms of the PLHRH in the convective sector. In this it may be seen that Ccond followed by Rcond are the most important contributions to heating the atmosphere. Ivan and Conson released large amounts of energy. In the regions surrounding the eye (first 30 km) it was possible to find peaks of Rcond of 3.0 K hr^{-1} in Conson and 6.5 K hr^{-1} in Ivan. Catarina showed peaks of heating of the order of only 1.5 K hr^{-1}. The mean values for Ivan, Conson and Catarina, were 1.5 K hr^{-1}, 1.0 K hr^{-1} and 0.8 K hr^{-1}, respectively.

As already pointed out, although the calculations clearly show large values of heating in Ivan, PR did not scan its most active sector. That is, the magnitude and horizontal extension of Ivan's heating rates Rcond and Ccond could be much greater than those of the other two systems.

The heating due to the vertical flux of frozen hydrometeors (Dep) had a profile similar to Rcond. Conson heated more the interior regions, and had magnitude similar to Catarina in the exterior regions. Ivan also heated more in the exterior regions (~0.04 K hr^{-1}) and this was related to the greater concentration of ice (Fig. 2).

The cooling due to melting of aggregates (Melt) was greater in the interior parts of the cyclones, where the convective towers were located. The magnitude of this term was less compared to the others terms. The minimum was found in the towers, where there was more ice to melt. In Conson this minimum was –0.17 K hr^{-1}, in Ivan it was –0.25 K hr^{-1} and in Catarina –0.08 K hr^{-1}.

The total heating (Total) shows the obvious. Although the scanning by TRMM lost the most active sector, the super-hurricane Ivan heated more the atmosphere around, especially in the spiral legs up to 60 km from its center. The magnitude was of the order of 5.0 K hr^{-1}. Conson had values of the order

of 3.0 K hr^{-1} and Catarina of 2.0 K hr^{-1} in their spiral rings. In the more interior parts of the rings, Conson was slightly more active than Ivan, showing values of the order 8.0 K hr^{-1}, while Ivan had magnitude of 6.0 K hr^{-1}, but with a strong peak (> 12 K hr^{-1}) at 20 km from the center. Catarina did not show any appreciable peak (Fig. 4), i.e, the heating in this storm was more uniform from the center through the borders.

Figure 5 shows the stratiform sector of the three systems. As already expected, Ccond values of up to 0.6 K hr^{-1} were found in Catarina, but without an appreciable peak. In Conson, the heating due to Ccond was large in the interior rings, where values of the order of 1.3 K hr^{-1} were found. Ivan had two peaks, one at 30-40 km from de center of the hurricane and the other between 120 and 150 km with magnitude of 1.0 K hr^{-1}. These differences were important and were directly related to the differences between distributions and magnitudes of water content.

The Dep term, like the Ccond, was proportional to ice content inside the system. Catarina had less ice, but showed a more uniform horizontal distribution (Fig. 3). So, the heating due to this hydrometeor was almost constant between 30 and 150 km from the center, with a magnitude of 0.03 K hr^{-1}. Conson had two peaks, like Ivan. In the vertical (not shown) the Dep term had a maximum between 4 and 6 km levels in Ivan and Conson, and 4 and 5 km in Catarina.

The DepI term showed a different behavior. Ivan had a maximum at 20 km (~1.9 K hr^{-1}) and another at 130 km (~0.4 K hr^{-1}). Conson had much more convective activity between 30 and 90 km, with a maximum at 60 km (~0.7 K hr^{-1}). This maximum was related to a strong area with deep convective activity in the NE sector (Fig. 1a). In the other sectors the magnitude of this term was similar to Catarina. Catarina did not show an appreciable peak, but was successful in heating the whole radial extension.

The cooling due the evaporation of cloud drops (Evap) showed new aspects. Ivan and Conson had more cooling in the internal rings, with values up to –0.55 K hr^{-1} and –0.45 K hr^{-1}, respectively. The cooling decreased in magnitude into the exterior rings in this cyclone, but Ivan showed another peak at 140 km. Catarina, cooling more between 40 and 90 km, had similar magnitude as those of the other two cyclones. This large rate of evaporation, probably, was related to a drier atmosphere above the cold ocean where the Catarina had originated and developed.

The melting term (Melt) had a behavior very similar to the Evap term in Conson and Ivan. The magnitude of this term was large at 30 km from the center of these two hurricanes (~-0.12 K hr^{-1}). Catarina did not show an appreciable peak, and cooled more the atmosphere between 30 and 90 km from the center.

Adding all terms (Total, eq. 14) it is possible to see that Catarina had a lower activity, also in the stratiform sector. The mean magnitude was 0.3 K hr^{-1} for Catarina against 0.6 K hr^{-1} for Conson and 0.8 K hr^{-1} for Ivan. The activity was more spatially uniform in Catarina, with small peaks of heating. The energy was more concentrated between 30 and 120 km. Ivan showed three peaks at 30, 90 and 130 km. These peaks were related to the conversion of vapor into cloud water (Ccond). Conson showed a strong heating between 30 and 90 km. The most important term in the stratiform sector was Ccond, followed by DepI.

6 – Hurricane Catarina

Hurricane Catarina whose genesis and evolution occurred in South Atlantic Ocean, not only caused damage in Santa Catarina coast, but also changed Brazilian meteorology. Fortunately, its almost continuous monitoring by satellites gave the chance to study this phenomenal hurricane in many ways. The data obtained from the TRMM satellite, more specifically the data from the Precipitation Radar, or PR, that crossed the hurricane three times during its lifetime is very useful for this study.

When the first crossing happened at 12:13 UTC on 24 march 2004 (Fig. 6, top panel), Catarina was in its formative stage. During two days it was seen as a low-pressure system, in the wake of a semi-stationary cold front over Brazil and the South Atlantic. In the PR/TRMM image it was already possible to see a strip of comma shaped cloudiness with reflectivity of 26-28 dBz at 3 km altitude. The convective center at the base of the comma presented a reflectivity of 35 dBz. At this moment Catarina was classified as a tropical storm. Catarina developed in a region of negative potential isentropic vorticity anomaly (Mattos and Satyamurty 2004) and with a strong zonal sea surface temperature (SST) gradient, which helped the system to deepen.

In the second crossing of TRMM at 06:11 UTC on 27 March (Fig. 6, center), in the early morning hours, all tropical hurricane characteristics were found. It was possible to see an eye, with 55 km of diameter, and two spiral bands. Hurricane Catarina had a zonal trajectory, following the maximum gradient of TSM, somewhat similar to the Australian coastal cyclones (Holland 1997). In the neighborhood of the Brazilian coast there was a positive anomaly of TSM. It was in this region hurricane Catarina gained strength and received the classification of category 1-2 hurricane. The last crossing of the satellite happened on the same day at 11:00 UTC (Fig. 6, bottom). Convective activity was seen over a large area and the eye had decreased in size.

Fig. 7 shows the azimuthal reflectivity profiles of stratiform and convective sectors. On 24 March (Fig. 7, top panel) the center of the system was situated at 29.15°S and 39.75°W. In the convective sector there was already a deep tower at 70 km from the center. This tower, which can also be seen in Fig. 6, was located at about 29°S and 39°W. It showed a mean reflectivity of nearly 40 dBz at the 2 km level, and was clearly visible at 10 km with a reflectivity of > 20 dBz. Probably this tower was deeper than shown here. But the PR is almost insensible to ice crystal, which has a very low dielectric constant, and therefore a very low reflectivity. The reflectivity was weaker in the periphery of the system.

Something similar was seen in the stratiform profile. The BB zone was approximately located at 3.7 km height at 90 km distance from the center. The BB height decreased gradually in the direction of its periphery, where it was situated at 3.3 km of height (180 km from the center). The inclination (~ 2.93 m km^{-1}) was a sign of hotter nucleus and cooler periphery.

On 23 March (1213 UTC) the convective towers were less deep, but were more active, especially on the periphery of the system. The maximum activity was restricted to the first 4 km of the troposphere and was possible to see many convective centers. The stratiform profile showed three regions with very pronounced BB, indicating large amounts of ice (at 60, 80 and 120 km). The BB had a slope of 2.30 m km^{-1} at this moment, with higher elevations near the center and lower elevations away from the center.

Twelve hours after the last passage the, TRMM took the last image of hurricane Catarina (Fig. 7, bottom). The region with strongest activity was concentrated in only one nucleus at 60 km away from the center. The reflectivity field was more homogeneous. The BB was not so visible as in the last two images. But it was still noted, especially between 50 and 90 km. The BB had a slope of 2.12 m km^{-1}, less than before, indicating that the periphery of the cyclone was warming and the center cooling.

a – Hydrometeor Profiles

Figure 8 shows the mean profiles of hydrometeors (rain and cloud water, aggregates and ice crystals). The convective profiles were given in the left column and the stratiform profile in the right column. In general, it is possible to see the growth of the rain water content with time. But this may be somewhat artificial because each measurement was taken in a different hour, and that the microphysical process was in different phases of its diurnal evolution.

In spite of the limitation, it is possible to say that there was an increase in rain water content between the 2 and 4 km levels between morning of 24 (Fig, 8, top) and the morning of 27 (Fig. 8,

bottom), comparing the measurements taken at almost the same local hour. Near the 3 km altitude the rain content was 0.3 g kg^{-1} (Fig. 8, bottom) in the convective sector and 0.07 g kg^{-1} in the stratiform sector. In the morning of 24 March these were 0.17 g kg^{-1} (convective) and 0.04 g kg^{-1} (stratiform). This was a response to the growth of aggregate content, especially in the convective sector, which is converted to rain after crossing the level of melting (0 °C).

The cloud water content changed very little during the whole lifetime of the hurricane. Between 2 and 4 km altitude, it had mean values of 0.09 g kg^{-1} in the convective sector and 0.025 g kg^{-1} in the stratiform sector. It might be a response to an almost constant conversion of water vapor to cloud water, as function of vapor concentration and environmental temperature.

The mean profile of ice content on stratiform sector remained almost invariable. At higher levels (above 7 km) the mean content was 0.05 g kg^{-1}. In the levels below 7 Km, the ice content decreased sharply. This decrease was associated with a lesser efficiency of the deposition process due to heterogeneous nucleation and diffusivity, which were more efficient at temperatures below –15°C, i.e., around 7 to 8 km.

Normally, the aggregate content, basically graupel and snow, grew sharply with the decrease of height, especially so in the stratiform sector where the growth was strong between 4 and 6 km. In the convective sector, only in the regions above and near the freezing level the growth of aggregate contents was large. In the first passage (Fig. 8, top) this showed a peak of 0.12 g kg^{-1} (as compared to 0.08 g Kg^{-1} in the stratiform sector) at the level of 4.0 km. In the second passage this value increased to 0.16 g kg^{-1} (as compared to 0.13 g Kg^{-1} in the stratiform sector) and later further increased to 0.23 g kg^{-1} (0.14 g Kg^{-1} in the stratiform sector) in the last passage. Between the first and the last observation, taken almost at the same local hour, but in different development phases of the system, the peak of aggregates, doubled in value at 4 Km. Both in convective and stratiform sectors. This continuous growth may be due to the availability of larger amounts of super-cooled drops collected and due to the entrainment of moist air in the levels above 5 km, in the final phase of the development.

b – PLHRH

Fig. 9 shows the profiles of some terms of the PLHRH. The convective sector profiles and the stratiform sector profiles are given in the left and the right columns, respectively, of the figure. In the beginning (Fig. 9, top), in Catarina, due to large crystal content, the atmosphere at the levels above the 8

km height was heated up (DepI term). The maximum stratiform heating rate varied from 0.75 to 1.0 K hr^{-1} and was associated with the presence of high and deep convective towers.

In the second passage of the TRMM (center panels), the convective sector showed little vertical development (Fig. 7, center panels). This was due to the local time of scanning (0600 HLT) and very little ice content. The stratiform profile was more active in this passage than in the previous passage, where there were some peaks of heating associated with the deposition of crystals (DepI) and condensation (Ccond). The evaporation of rainwater was strongest in this profile than in the last profile. Probably, this activity was related to the residual activity of the convective tower growth during the previous night.

In the third passage (Fig 9, bottom) the convective sector was more active. This relatively higher rate of heating (larger than 0.8 K hr^{-1} at levels below 5 km) was associated not with the presence of deep convective tower, as in the first passage, but to a more homogeneous horizontal distribution of the areas with convective activity that grew along the day. In the stratiform sector the profile was similar to the previous passage.

The aggregate content was very low during the first passage that resulted in a relatively low heating rate at all levels above the melting level. The evolution of this profile was almost the same as the ice aggregates content. In the last passage, the heating rate was about 0.05 K hr^{-1} (convective) at 4.5 km, however decreasing to almost zero at 5.5 km. In the stratiform sector this heating was also small, but extended to the whole atmospheric column above the melting level.

The cooling due the melting (Melt) of ice was limited to the first kilometer below the melting level, in the stratiform sector as well as in the convective sector. This remained almost without change in the last two passages.

The heating due the rainwater flux (Rcond) also showed some variation in the convective sector, around 0.4 K hr^{-1} below 4.0 km. The Rcond term showed a relative increase, especially between the first and the third passages, taken at almost the same local time. In the last passage there was a maximum heating rate immediately below the melting level. The cooling due to evaporation of rain water (Evap term, in the stratiform) had a mean magnitude of about –0.25 K hr^{-1} in the three passages, but increasing to –0.5 K hr^{-1} at levels below 3 km.

Figure 10 shows the total *PLHRH* for the convective and stratiform sectors and the sum of the two. At first, the predominance of stratiform sector was clear. Despite that the convective sector had a greater magnitude with values of the order of 1.0 to 1.2 K hr^{-1}, the area covered by the stratiform sector

was 20 to 30% larger. The heating profile was clearly bi-modal, with a peak at the 4.5 km level, i.e. at 600 hPa, and another at 8 km or above. This occurs for large values of relative humidity and low temperatures, or yet within convective domes, where the cooling can be compensated by the heating in other stratiform areas (Ccond term) and convective ones (Rcond e Ccond terms). The bi-modal profile can be found in mature convective cells (Tao et al. 1990, 1993), as observed in a mesoscale convective complexes and squall lines in the USA, as an apparent heat source (Grell et al. 1991) and in the 1970-2000 climatology over the Amazon (Paixão Veiga et al. 2005).

Despite that the convective sector intensified during the evolution of the system, the magnitude of total heating did not change much. In the first passage, mean values of heating at low levels were of the order of 1.0 K hr^{-1}, whereas in the other two passages it was 1.5 K hr^{-1}, approximately. There were large rates of heating at higher levels also due to ice deposition (represented by DepI), with values of 3.0 K hr^{-1} in the last passage (Fig. 10, bottom).

7 – Conclusions

The present work analyzed the hydrometeor and latent heat profiles adapting a model by Tao et al. (1990) and PR/TRMM reflectivity data. Usually, the latent heat is estimated as a residual of the thermodynamic equation. In the present study, it was directly estimated from hydrometeor profiles. Solid hydrometeors were estimated from the method developed by Heymsfield (2003) and, liquid hydrometeors from Ulbrich (1983), Dou et al. (1999) and Viltard et al. (2000).

These methods were applied to study two tropical hurricanes and one subtropical, namely hurricane Catarina that was considered a severe event for Brazilian standards, though very weak cyclone when compared to average hurricanes and typhoons in the Northern Hemisphere. The origin and evolution of hurricane Catarina was somewhat similar to the ones analyzed by Holland et al. (1987) in the Australian east coast. Hurricane Catarina was a shallow system with less ice and water contents. It was colder and was found to have a BB 1000 m below the level found in other two systems analyzed here. Moreover, the BB showed a large slope, being higher near its center. This was an indicative of a warm core.

High mean water content was found in Conson and Ivan at low levels and closer to the center of the hurricanes. In Catarina there was less water and was more concentrated between 30 and 90 km from the center. The mean ice content in Catarina was of the order of 0.05 g kg^{-1}, while in Conson it was 0.06

g kg^{-1} and in Ivan 0.08 g kg^{-1}. Conson and Ivan cyclones recorded water content values of up to 0.3 g kg^{-1} in areas located above the melting layer, while Catarina had maximum value no greater than 0.15 g kg^{-1} in the same region. That is, Catarina had only half the amount of water observed in the Northern Hemisphere hurricanes.

Due the differences between geographical location and dynamical origins, each hurricane had its own hydrometeor and heating profile. Conson and Ivan were very similar both in origins as in evolution, even considering the great distance between them. So, similarities between hydrometeor and heating profiles were expected. The Catarina was atypical, originating from an extratropical disturb whose the amount of water and ice content (almost an order of magnitude (Heymsfield, 2003)) is lesser than a tropical system. Errors in the water and ice contents related to a simple correlation between reflectivity and hydrometeor (Table 2) can't be avoid but may be still useful if was considered the large variability of the parameters involved in a DSD relationship (Viltard et al, 2000) and the impossibility to decide which one is more correct between these relations (Straka et al, 2000). How was already demonstrated in others studies, usually the heating profiles are very sensitive to classification between convective and stratiforme (Lang et al, 2003) and the temperature (Liu and Fu, 2001).

Some heating terms (Rcond and Melt in convective regions and Evap, Dep and DepI in stratiform regions) in Catarina showed magnitudes similar to the other hurricanes. Greater differences were restricted to regions near the eye. The heating profiles in the three systems agreed with those found in others studies (Tao et al. 1990, Tao et al. 1993, Yang and Smith 1999). However, they differ in magnitude and the low heating rates between the 5 and 6 km levels.

The present method is physically sound and straight forward. Furthermore, stratiform and convective latent heat profiles can be easily distinguished. Further work is underway to apply the method to initiate numerical weather models.

Bibliography

Anagnostou, E. N., C. A. Morales, and T. Dinku, 2001: The Use of TRMM Precipitation Radar Observations in Determining Ground Radar Calibration Biases. J. Atmos. Oc. Tech., 18, 616-618.

Beard, K. V., and S. N. Grover, 1974: Numerical Collision Efficiencies for small raindrops colliding with micron size particles J. Atmos. Sci., 31, 543-549.

Bolen, S. M., and V. Chandrasekar, 2000: Quantitative Cross Validation of Space-Based and Ground-Based Radar Observations. J. Appl. Meteorol., 39(12), 2071–2079.

Brown, J. M., 1979: Mesoscale Unsaturated downdrafts Driven by Rainfall Evaporation: A Numerical Study. J. Atmos. Sci., 36, 313-338.

Calearo, D., G. Araújo, C. Correa, M. Moraes, M. L. Rodrigues, M. Monteiro, M. Martins, R. Victoria, and C. E. Araújo, 2004: Monitoramento do Catarina no Centro Operacional da EPAGRI/CLIMERH. Anais do XIII Congresso Brasileiro de Meteorologia. Fortaleza. Fortaleza. In Portuguese. Available from Sociedade Brasileira de Meteorologia, www.sbmet.org.br, Rio de Janeiro, Brazil.

Chandrasekar, V., and V. N. Bringi, 1987: Simulation of Radar Reflectivity and Surface Measurements of Rainfall. J. Atmos. Oc. Tech., 4, 464–478.

DeMaria, M., 1985: Linear Response of a Stratified Tropical Atmosphere to Convective Forcing. J. Atmos. Sci., 42, 1944–1959.

Dou, X., J. Testud, P. Amayenc, and R. Black, 1999: The concept of normalized gamma distribuition to describe raindrop spectra, and its use to parameterize rain relations. 29th Int. Conference on Radar Meteorology, Montreal, Quebec, Canada, Amer. Meteorol. Soc., 625-628.

Gagin, A., 1971: Studies of factors governing the collidal stability of continental clouds, Int. Conf. on Weather Modification, Canberra, Australia, Amer. Meteor. Soc., 5-11.

Gandu, A. W., and J. E. Geisler, 1991: A Primitive Equations Model Study of the Effect of Topography on the Summer Circulation over Tropical South America. J. Atmos. Sci. 48, 1822-1836.

Gandu, A. W., and P. L. Silva Dias, 1998: Impact of Tropical Heat Sources on the South American Tropospheric upper Circulation and Subsidence. J. Geophys. Res., 103, N° D6, 6001-6015.

Grell, G. A., Y.-H Kuo, and R. J. Pach, 1991: Semiprognostic Tests of Cumulus Parameterization Schemes in the Middle Latitudes. Mon. Wea. Rev., 119, 5-31.

Gusso, A., 2004: Preliminary physical aspects of extra-tropical cyclone Catarina-1 at perspective of NOAA satellite data. Fortaleza. In Portuguese. Available from Sociedade Brasileira de Meteorologia, www.sbmet.org.br, Rio de Janeiro, Brazil.

Heymsfield, G. M., B. Greerts, and L. Tian, 2000: TRMM Precipitation Radar Reflectivity Profiles as Compared with High-Resolution Airborne and Ground-Based Radar Measurements. J. Appl. Meteorol., 39, 2080-2112.

Heymsfield, G. M., 2003: Properties of Tropical and Midlatitudes Ice Cloud Particle Ensembles. Part II: Applications for Mesoscale and Climate Models. J. Atmos. Sci., 60, 2592-2611.

Holland, G. J., A. H. Linch, and L. M. Leslie, 1987: Australian East-Coast Cyclones. Part I: Synoptic Overview and Case Study. Mon. Wea. Rev., 115, 3024-3036.

Iguchi, T., T. Kozu, R. Meneghini, and J. Awaka, K. Okamoto, 2000: Rain-Profiling Algorithm for the TRMM Precipitation Radar. J. Appl. Meteorol., 39, 2038-2028.

Kummerow, C., W. Barnes, T. Kozu, J. Shiue, and J. Simpson, 1998: The Tropical Rainfall Measuring Mission (TRMM) Sensor Package. J. Atmos. Oc. Tech., 15, 809–817.

Lang, S., W.-K. Tao, J. Simpson, and B. Ferrier, 2003: Modeling of Convective–Stratiform Precipitation Processes: Sensitivity to Partitioning Methods. J. Appl. Meteorol., 42, 505–527.

Leary, C. A., and R. A. Houze Jr., 1979: Melting and Evaporation of Hydrometeors in Precipitation from the Anvil Clouds of Deep Tropical Convection. J. Atmos. Sci., 36, 669-679.

Li1ly, D. K. 1964: Numerical Solutions for the Shape-Preserving Two-Dimensional Thermal Convection Element. J. Atmos. Sci., 21, 83–98.

Liu, G., and Y. Fu, 2001: The Characteristics of Tropical Precipitation Profiles as Inferred from Satellite Radar Measurements. J. of the Meteorol. Soc. of Japan, 79(1), 131-143.

Mattos, L. F., and P. Satyamurty, 2004: Catarina: A rare system on the coast of Brazil. Proceedings of XIII Brazilian Meteorological Conference. Fortaleza. In Portuguese. Available from Sociedade Brasileira de Meteorologia, www.sbmet.org.br, Rio de Janeiro, Brazil.

Olson, W. S., C. D. Kummerow, S. Yang, G. W. Petty, W.-K Tao, T. L. Bell, S. A. Braun, Y. Wang, S. E. Lang, D. E. Johnson, and C. Chiu, 2006: Precipitation and latent heating distribuitions from satellite passive microwave radiometry. Part I: Method and uncertainties. J. Appl. Meteorol., 45, 702-720.

Paixão Veiga, J. A., V. Brahmananda Rao, S. H. Franchito, 2005: Heat and Moisture Budgets of the walker circulation and associated rainfall anomalies during el Niño events. Int. J. Climatol. 25, 193-213.

Pereira Filho, A. J., and R. S. Lima, 2006: Synoptic and mesoscale analysis of hurricane Catarina, Brazil. *Proceedings of the 8th International Conf. on Southern Hemisphere Meteorology and Hydrology*, Foz do Iguaçu. CDROM, Amer. Meteorol. Soc., Boston, USA.

Rocco, M. R., 2003: Caracterização Microfísica de Sistemas Precipitantes durante o Experimento WET/AMC TRMM/LBA. Dissertation thesis, São Paulo, Universidade de São Paulo.

Silva Dias, P. L., H. W. Schubert, and M. DeMaria, 1983: Large-Scale Response of the Tropical Atmosphere to Transient Convection. J. Atmos. Sci., 40, 2689–2707.

Silva Dias, M. A. F., S. Rutlege, P. Kabat, P. L. Silva Dias, C. Nobre, G. Fish, A. J. Dolman, E. Zipser, M. Garstang, A. O. Manzi, J. D. Fuentes, H. R. Rocha, J. Marengo, A. Plana-Fattori, L. D. A. Alvalá, M. O. Andreae, P. Artaxo, R. Gielow and L. Gatti, 2002: Cloud and rain processes in the biosphere-atmosphere interaction context in the Amazon Region. J. Geophys. Res., 107, NO. D20, 8072, LBA 39, 1-17.

Smith Jr., P. L., C. G. Myers, and H. D. Orville, 1975: Radar Reflectivity Factor Calculations in Numerical Cloud Models Using Bulk Parametrization of Precipitation. J. Appl. Meteorol., 14, 1156-1165.

Smith Jr., P. L., 1984: Equivalent Radar Reflectivity Factors for Snow and Ice Particles. J. Appl. Meteorol., 23, 1258-1260.

Smith, E. A., X. Xiang, A. Mugnai, and G. J. Trípoli, 1994: Design of an Inversion-Based Precipitation Profile Retrieval Algorithm Using an Explicit Cloud Model for Initial Guess Microphysics. Meteorol. Atmos. Phys., 54, 53-58.

Steiner, M., R. A. Houze, and S. E. Yuter, 1995: Climatological Characterization of Three-Dimensional Storm Structure from Operational Radar and Rain Gauge Data. J. Appl. Meteorol., 34, 1978–2007.

Straka, J. M., D. S. Zrnic, and A. V. Ryzhkov, 2000: Bulk Hydrometeor Classification and Quantification using Polarimetric Radar Data : Synthesis of Relations. J. Appl. Meteorol., 39, 1341–1372.

Tao, W. K., J. Simpson, S. Lang, M. McCumber, R. Adler, and R. Penc, 1990: An Algorithm to Estimate the Heating Budge from Vertical Hydrometeor Profiles. J. Appl. Meteorol., 29, 1232-1244.

Tao, W. K., 1993: The Goddard Cumulus Ensemble Model. Part I: Model Description. Terr. Atmos. Oceanic Sci., 4, 35-72.

Tao, W. K.; S. Lang, J. Simpson, and R. Adler, 1993: Retrieval Algorithms for Estimating the Vertical Profiles of Latent-Heat Release - Their Applications for TRMM. J. Meteorol. Soc. Japan., 71, 685-700.

Ulbrich, C. W., 1983: Natural Variations in the Analytical Form of the Raindrop Size Distribution. J. Clim. Appl. Meteorol., 22, 1764-1775.

Viltard, N., C. Kummerow, W. S. Olson, and Y. Hong, 2000: Combined Use of the Radar and Radiometer of TRMM to Estimate the Influence of Drop Size Distribution on Rain Retrievals. J. Appl. Meteorol., 39(12), 2103–2114.

Yanai, M., and Tomita, T. 1998: Seasonal and Interannual Variability of Atmospheric Heat Sources and Moisture Sinks as Determined from NCEP–NCAR Reanalysis. Journal of Climate, 11, 463–482.

Yang, S., and E. A. Smith, 1999a: Moisture Budget Analysis of TOGA COARE Area Using SSM/I-Retrieved Latent Heating and Large-Scale Q_2 Estimates. J. Atmos. Oc. Tech., 16, 633-655.

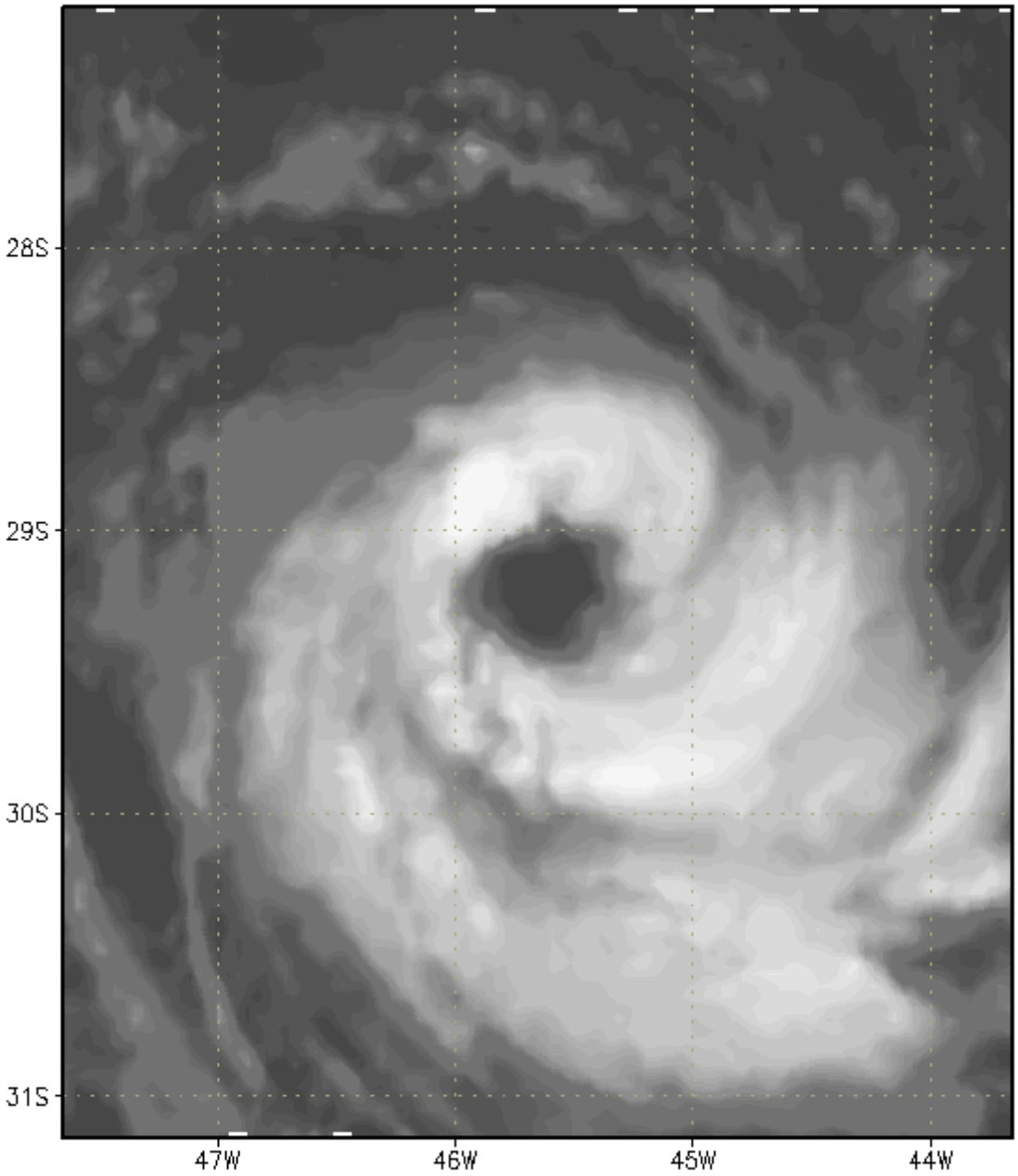

Fig. 1 - Infrared images of Conson on 08 Jun 2004 at 16:30 UTC (A), Ivan on 11 Sep 2004 at 1350 UTC (B) and Catarina on 27 Mar 2004 at 06:11 UTC (C).

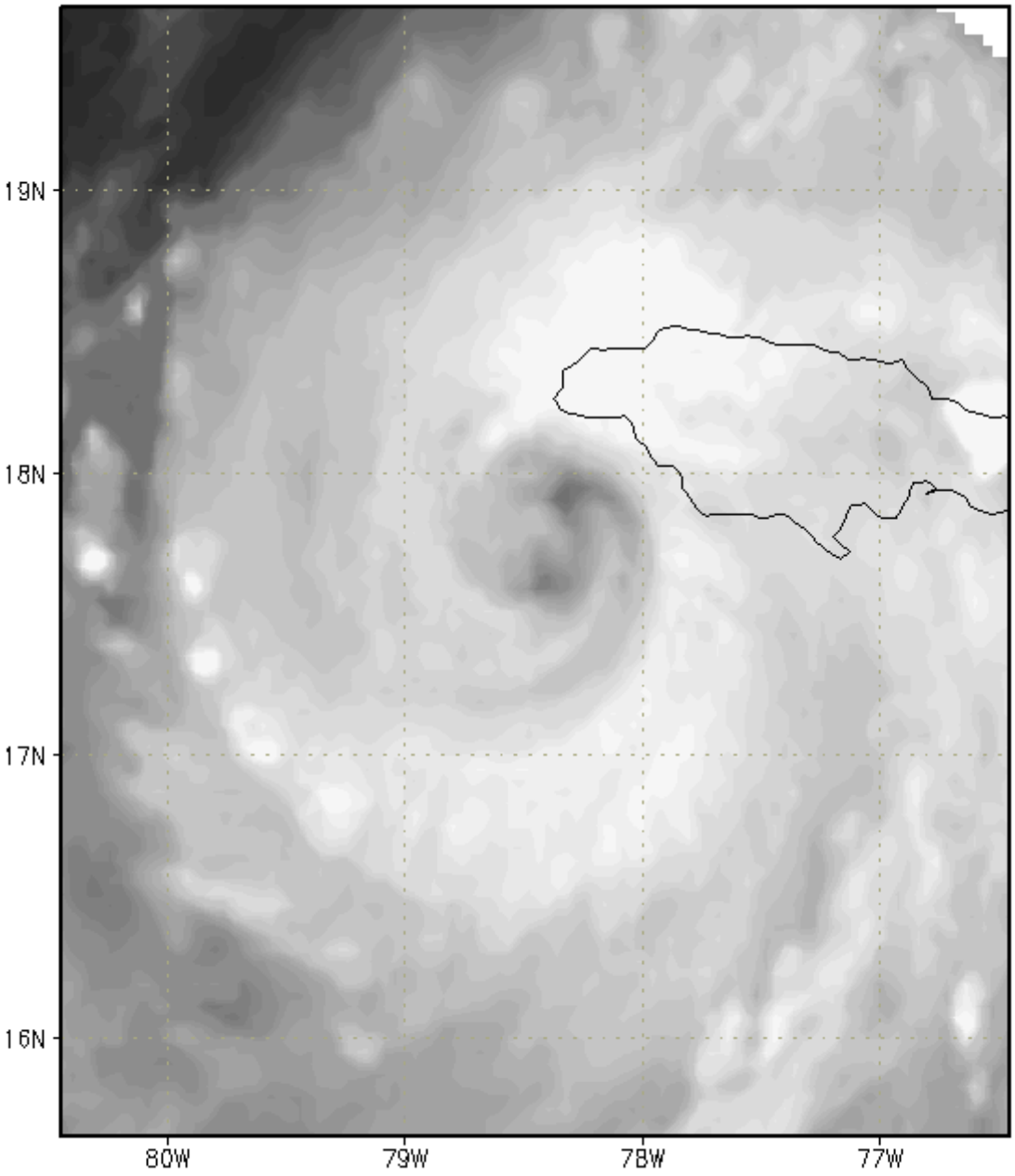

Fig. 1 - Continued

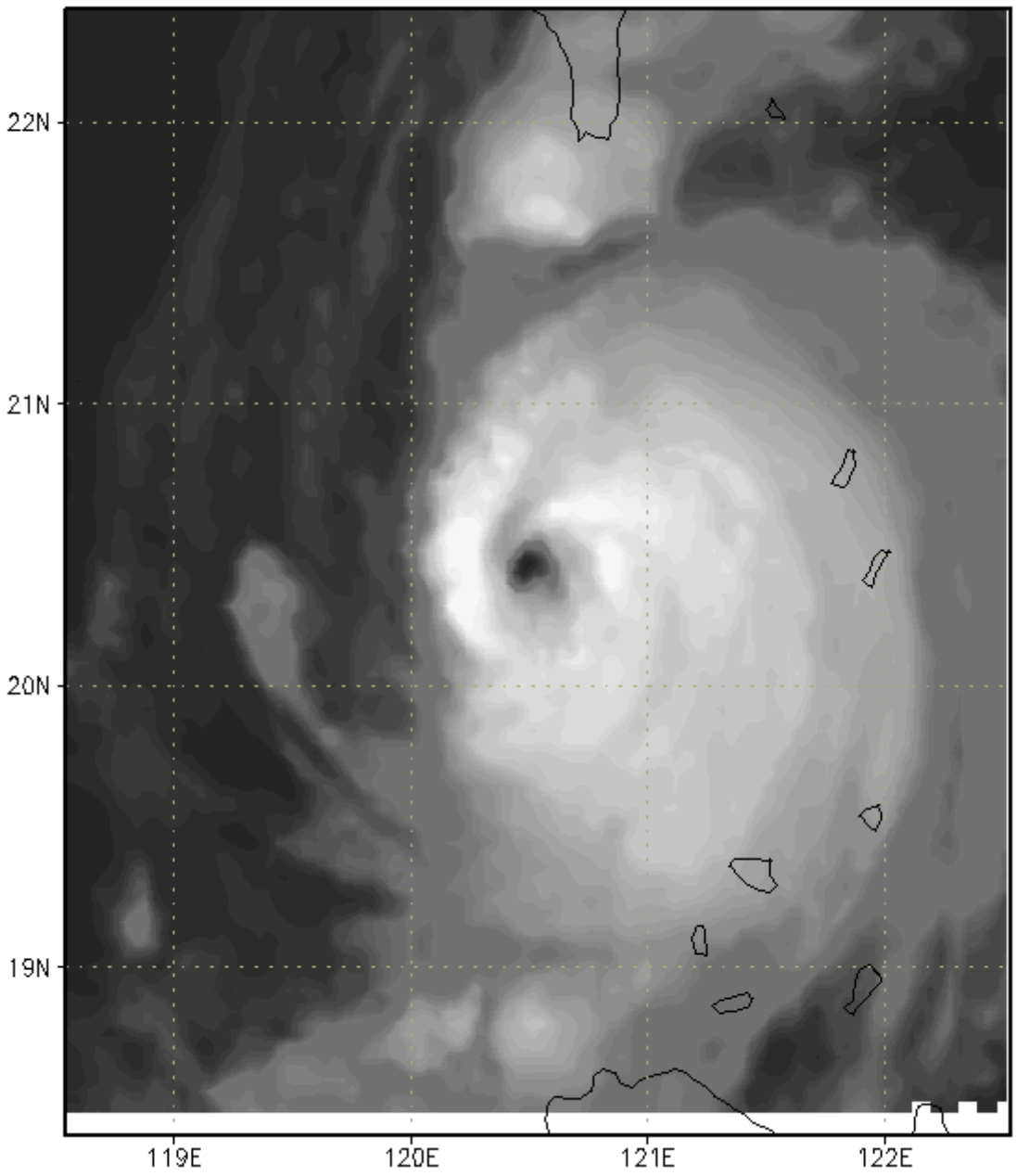

Fig. 1 - Continued

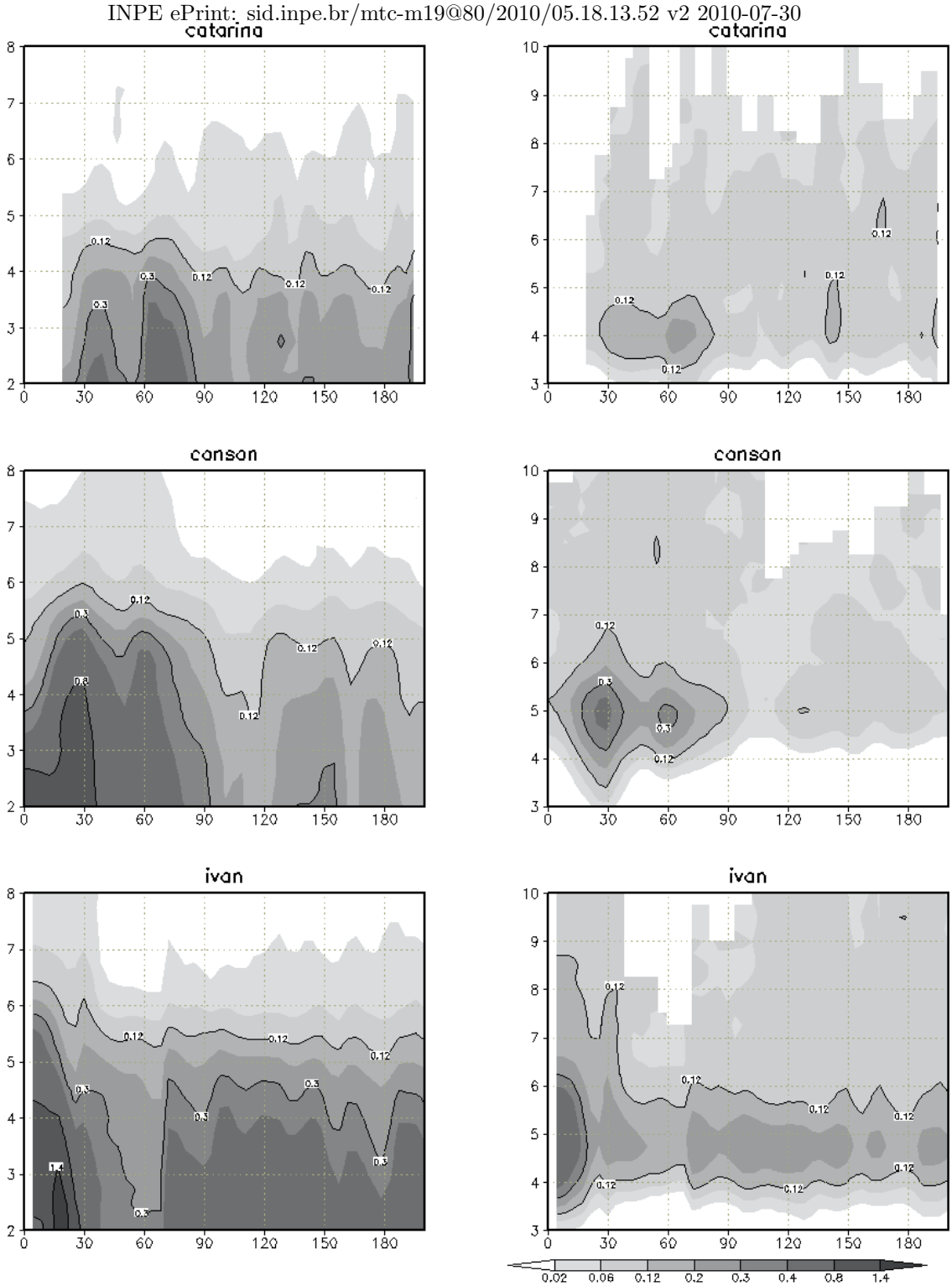

Fig. 2 - Azimutally averaged profiles from convective sector showing the water content (left column) and ice content (right column) of Catarina (top), Conson (center) and Ivan (bottom). Vertical and horizontal scale is in km and the water content in g kg^{-1}.

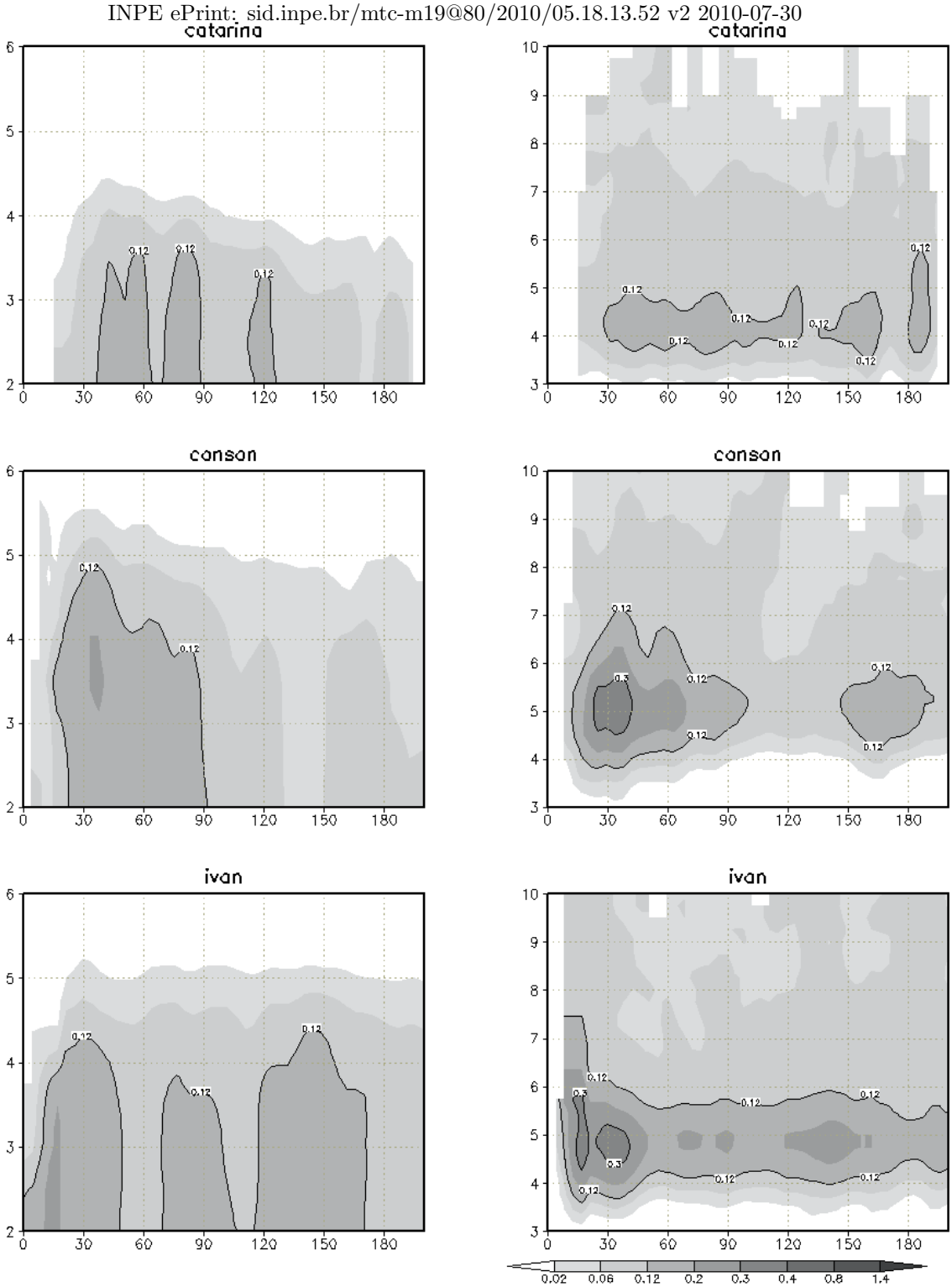

Fig. 3 - As in Figure 2 except for stratiform sector.

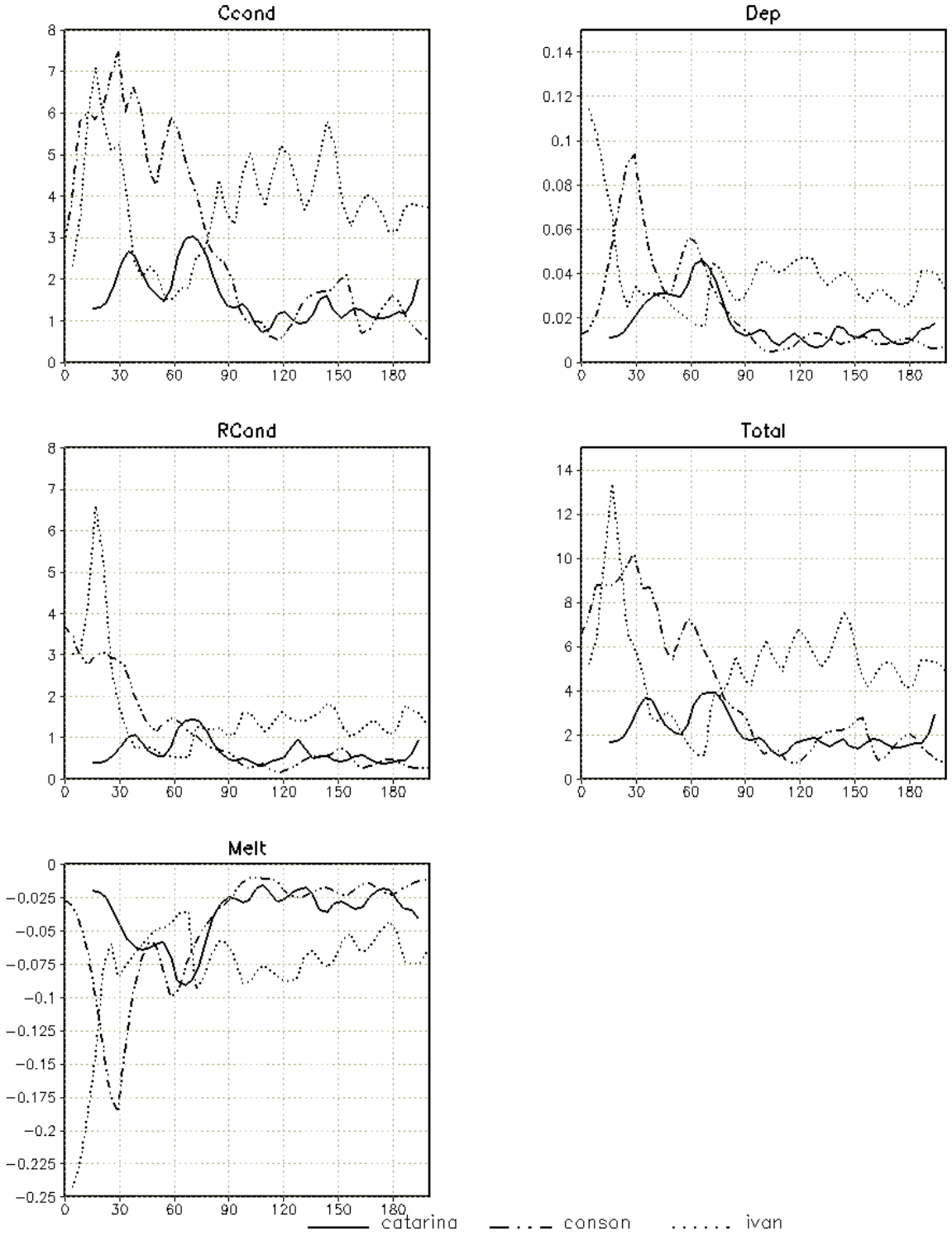

Fig. 4 - Azimuthal mean of the most important terms from the PLHRH integrated in the vertical in the convective sector. Units: K s^{-1}.

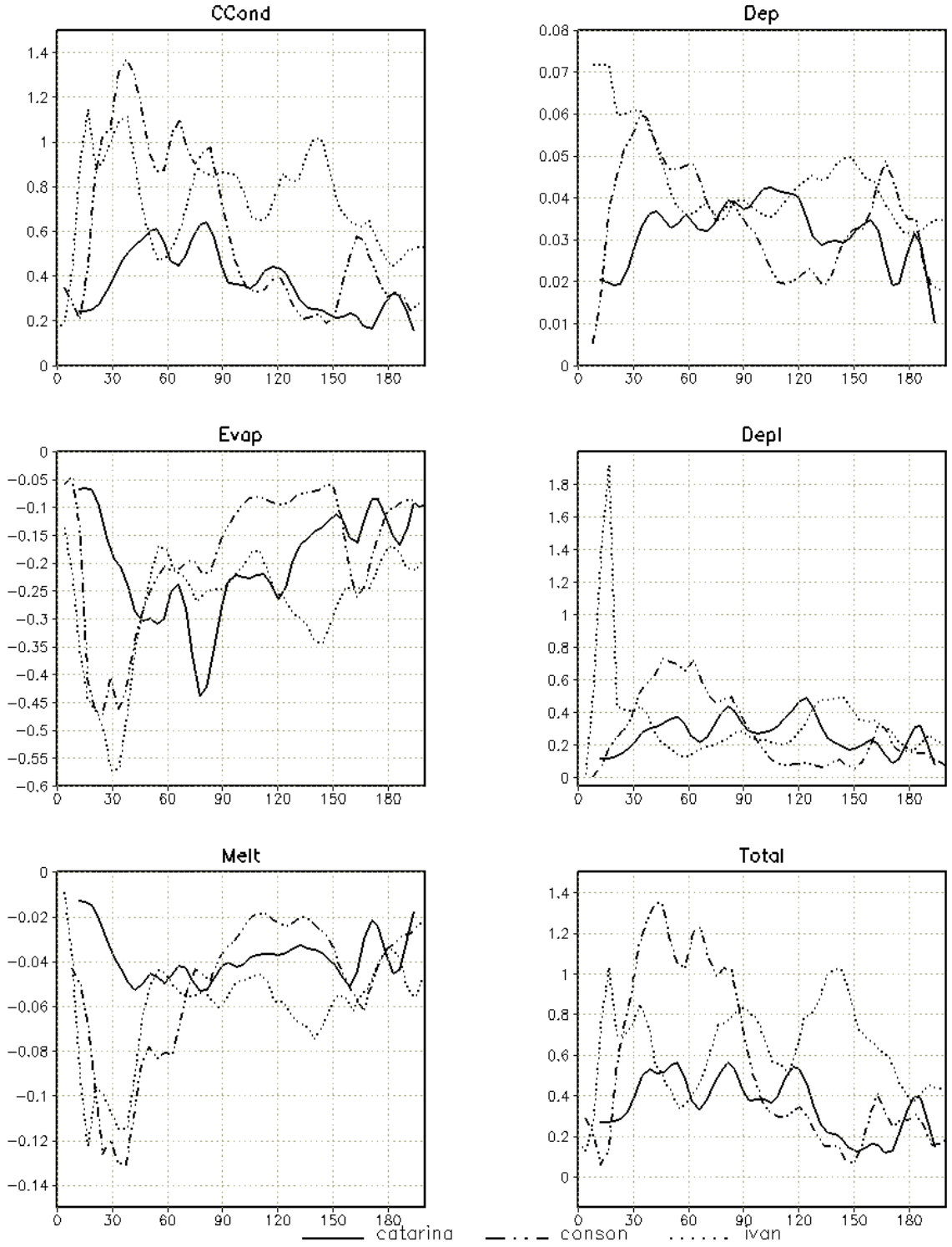

Fig. 5 - As in Figure 4, except for stratiform sector.

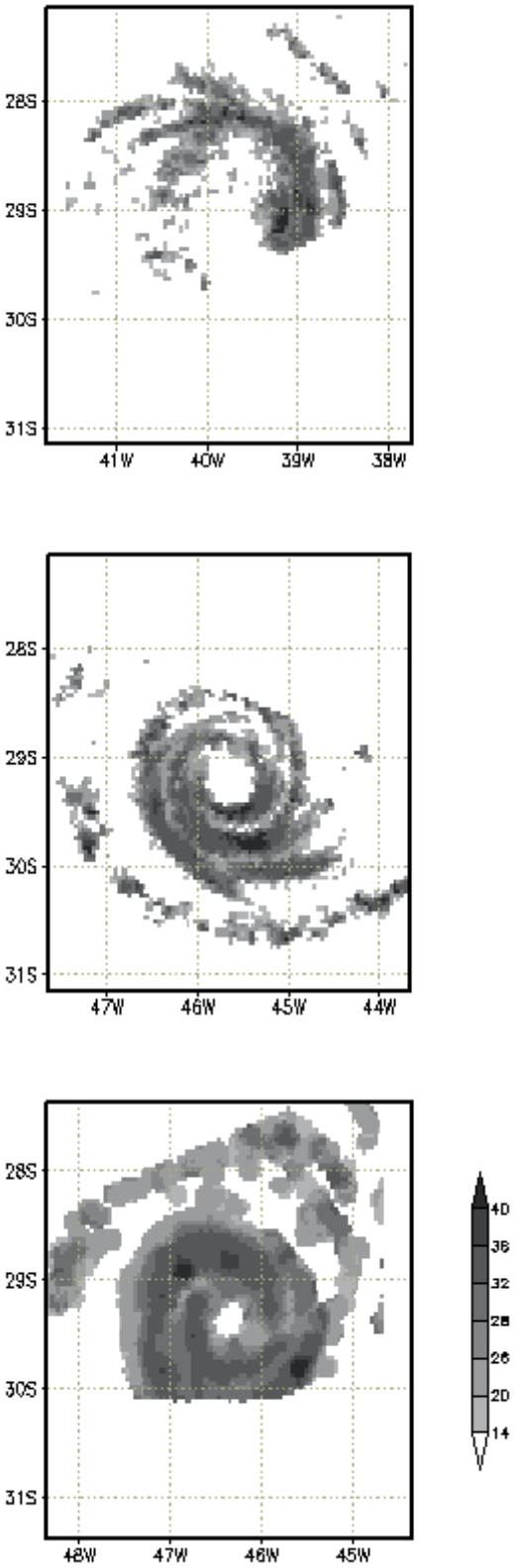

Fig. 6 – CAPPI of 3 km altitude taken on 24 Mar 2004 at 12:13 (top) and on 27 Mar at 06:11 (center) and 11:00 (bottom) of Catarina Cyclone.

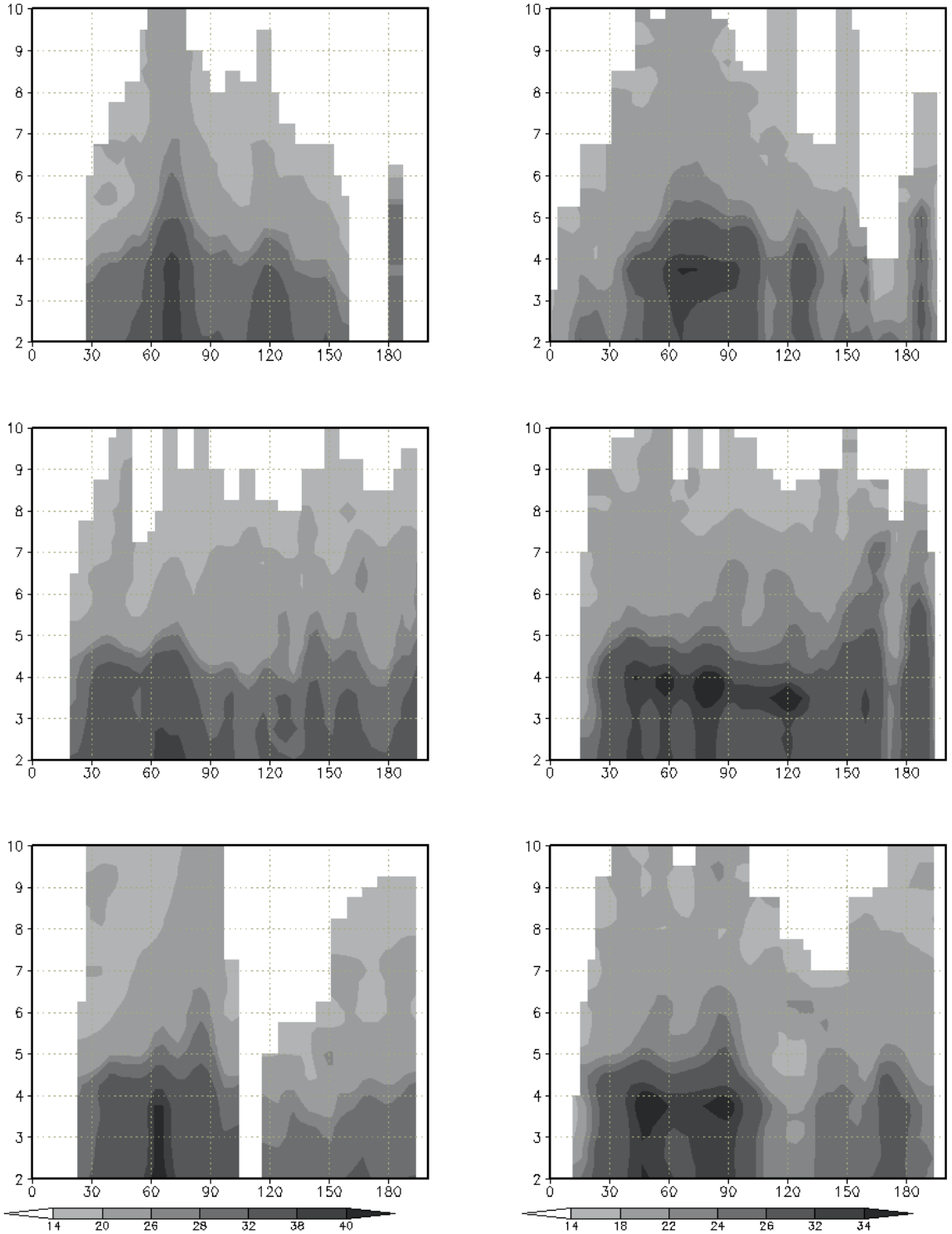

Fig. 7 – Azimuthally averaged profile of the convective reflectivity (left column) and stratiform reflectivity (right column) of Catarina Hurricane on 24 March 2004 at 1213 UTC (top) and on 27 Mar at 0611 UTC (center) and at 1100 UTC (bottom). Vertical and horizontal scales are in km and the reflectivity in dBz.

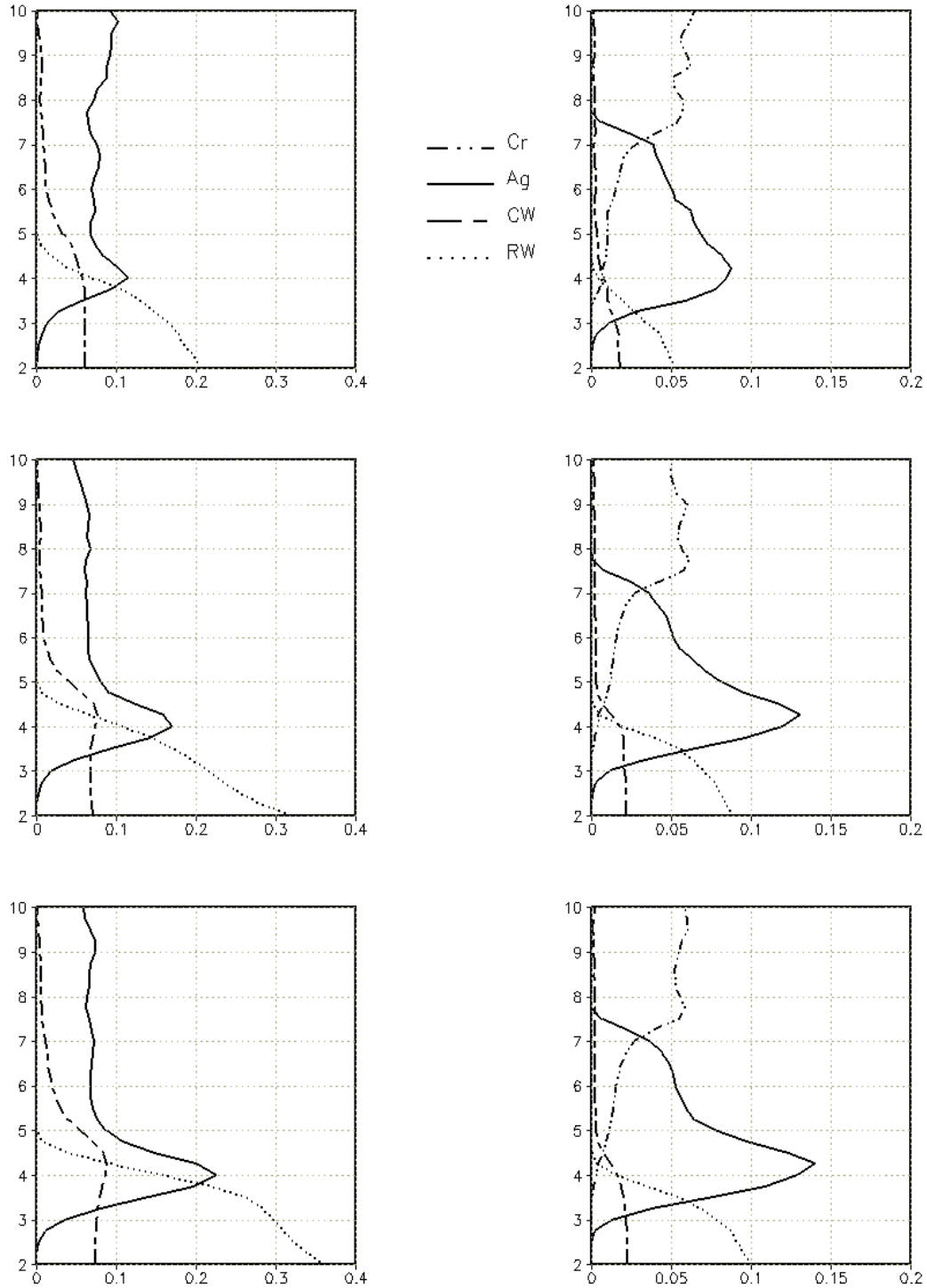

Fig. 8 - Hydrometeor mean profiles of rain water (RW) and cloud water (CW), aggregates (Ag) and ice crystals (Cr) for convective sector (left column) and stratiform sector (right column) taken on 24 Mar 2004 at 12:13 (top) and on 27 Mar at 06:11 (center) and 11:00 (bottom) of Catarina Cyclone. The vertical scale is in km. Unit: g kg^{-1}.

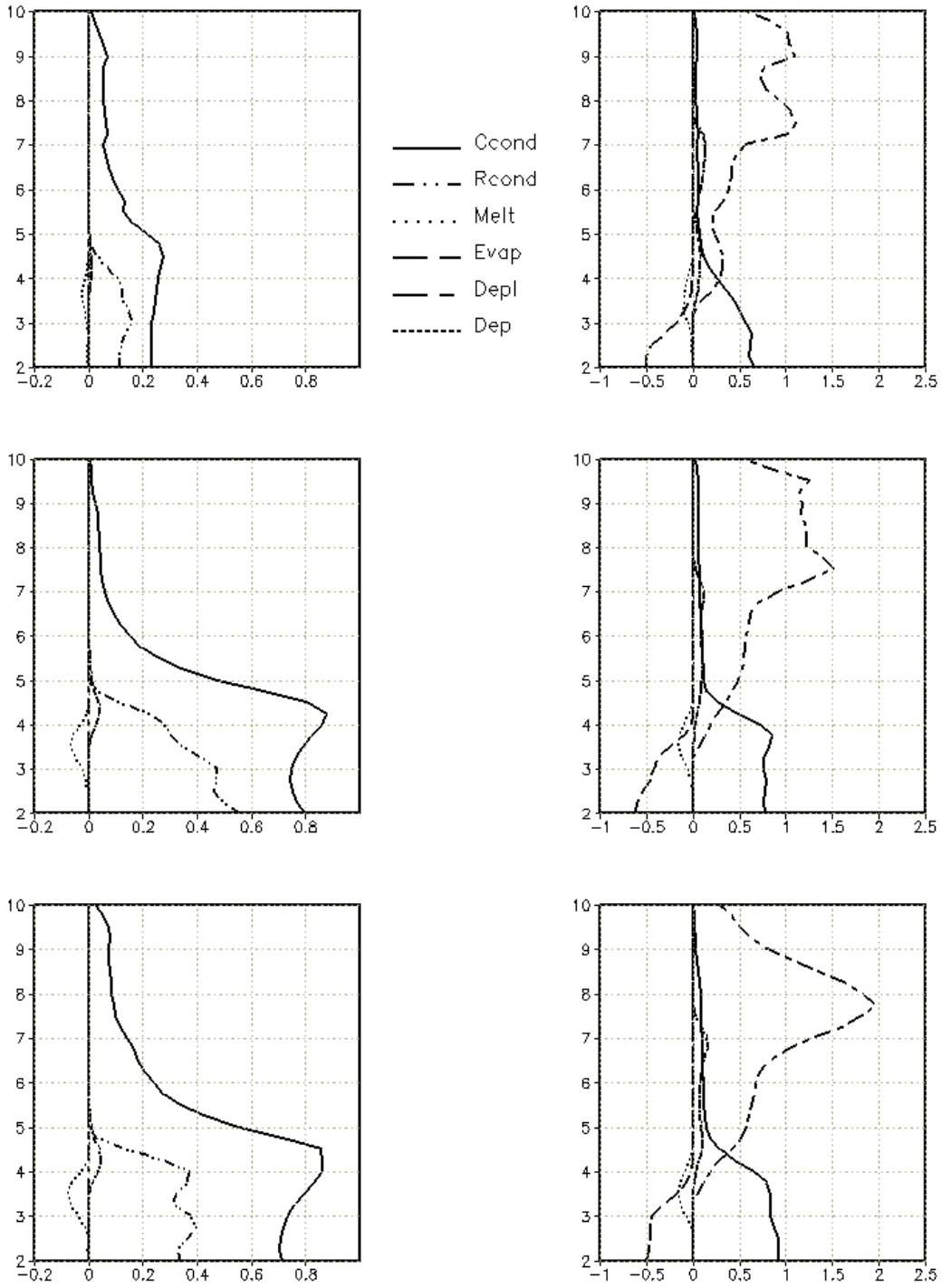

Fig. 9 – PLHRH mean profiles for convective sector (left column) and stratiform sector (right column) taken on 24 Mar 2004 at 12:13 (top) and on 27 Mar at 06:11 (center) and 11:00 (bottom) of Catarina Cyclone. The vertical scale is in km. Units: K hr^{-1}.

Fig. 10 – Profiles of convective heating (CVC), stratiform heating (STR) and total (TOTAL) obtained on 24 Mar 2004 at 12:13 (top) and on 27 Mar at 06:11 (center) and at 11:00 (bottom) of Catarina Cyclone. The vertical scale is in km. Units: K hr^{-1}.